Enhancing the signal-to-noise ratio of an infrared photodetector with a circular metal grating

Ravi D. R. Bhat[1], Nicolae C. Panoiu[2], Steven R. J. Brueck[3], and Richard M. Osgood, Jr.[1]

[1]*Department of Applied Physics and Applied Mathematics, Columbia University, New York, New York 10027, USA*
[2]*Department of Electronic and Electrical Engineering, University College London, Torrington Place, London WC1E 7JE, UK*
[3]*Center for High Technology Materials, University of New Mexico, Albuquerque, New Mexico 87106, USA*
rbhat@cumsl.msl.columbia.edu

Abstract: We use finite-difference time-domain (FDTD) simulations to demonstrate enhanced infrared absorption in a photodetector covered with a microstructured metal film consisting of a metal-plasmon grating collector/concentrator and sub-wavelength detector well; for circular gratings we use radial FDTD, and for linear gratings we use two-dimensional FDTD. We identify a figure of merit to quantify the improvement in signal-to-noise ratio of such a detector scheme. We optimize grating parameters for a circular grating surrounding a simple hole, showing that the signal-to-noise ratio can be improved by a factor of as much as 5.2, whereas the signal-to-noise improvement for comparable linear gratings is at most 1.7. In the case of the circular grating, this result is achieved with more than 400 times as much light absorbed in the hole as with a metal film but no grating.

OCIS codes: (240.6690) Surface waves; (230.5160) Photodetectors (050.1220) Apertures.

References and links

1. T. Thio, K. M. Pellerin, R. A. Linke, H. J. Lezec, and T. W. Ebbesen, "Enhanced light transmission through a single subwavelength aperture," Opt. Lett. **26**, 1972–1974 (2001).
2. T. Thio, H. J. Lezec, T. W. Ebbesen, K. M. Pellerin, G. D. Lewen, A. Nahata, and R. A. Linke, "Giant optical transmission of sub-wavelength apertures: physics and applications," Nanotechnology **13**, 429–432 (2002).
3. H. J. Lezec, A. Degiron, E. Devaux, R. A. Linke, L. Martín-Moreno, F. J. García-Vidal, and T. W. Ebbesen, "Beaming light from a subwavelength aperture," Science **297**, 820–822 (2002).
4. A. Nahata, R. A. Linke, T. Ishi, and K. Ohashi, "Enhanced nonlinear optical conversion from a periodically nanostructured metal film," Opt. Lett. **28**, 423–425 (2003).
5. S. Shinada, J. Hashizume, and F. Koyama, "Surface plasmon resonance on microaperture vertical-cavity surface-emitting laser with metal grating," Appl. Phys. Lett. **83**, 836–838 (2003).
6. F. I. Baida, D. Van Labeke, and B. Guizal, "Enhanced confined light transmission by single subwavelength apertures in metallic films," Appl. Opt. **42**, 6811–6815 (2003).
7. A. Degiron and T. W. Ebbesen, "Analysis of the transmission process through single apertures surrounded by periodic corrugations," Opt. Express **12**, 3694–3700 (2004).
8. H. J. Lezec and T. Thio, "Diffracted evanescent wave model for enhanced and suppressed optical transmission through subwavelength hole arrays," Opt. Express **12**, 3629–3651 (2004).
9. T. Ishi, J. Fujikata, and K. Ohashi, "Large optical transmission through a single subwavelength hole associated with a sharp-apex grating," Jpn. J. Appl. Phys. **44**, L170–L172 (2005).

#91481 - $15.00 USD Received 8 Jan 2008; revised 19 Feb 2008; accepted 20 Feb 2008; published 19 Mar 2008

10. E. Popov, M. Nevière, A.-L. Fehrembach, and N. Bonod, "Optimization of plasmon excitation at structured apertures," Appl. Opt. **44**, 6141–6154 (2005).
11. E. Popov, M. Nevière, A.-L. Fehrembach, and N. Bonod, "Enhanced transmission of light through a circularly structured aperture," Appl. Opt. **44**, 6898–6904 (2005).
12. C. K. Chang, D. Z. Lin, C. S. Yeh, C. K. Lee, Y. C. Chang, M. W. Lin, J. T. Yeh, and J. M. Liu, "Similarities and differences for light-induced surface plasmons in one- and two-dimensional symmetrical metallic nanostructures," Opt. Lett. **31**, 2341–2343 (2006).
13. K. L. Shuford, M. A. Ratner, S. K. Gray, and G. C. Schatz, "Finite-difference time-domain studies of light transmission through nanohole structures," Appl. Phys. B: Lasers Opt. **84**, 11–18 (2006).
14. J. Olkkonen, K. Kataja, and D. G. Howe, "Light transmission through a high index dielectric hole in a metal film surrounded by surface corrugations," Opt. Express **14**, 11506–11511 (2006).
15. C.-K. Chang, D.-Z. Lin, C.-S. Yeh, C.-K. Lee, Y.-C. Chang, M.-W. Lin, J.-T. Yeh, and J.-M. Liu, "Experimental analysis of surface plasmon behavior in metallic circular slits," Appl. Phys. Lett. **90**, 061113 (2007).
16. H. Cao, A. Agrawa, and A. Nahata, "Controlling the transmission resonance lineshape of a single subwavelength aperture," Opt. Express **13**, 763–769 (2005).
17. A. Agrawal, H. Cao, and A. Nahata, "Time-domain analysis of enhanced transmission through a single subwavelength aperture," Opt. Express **13**, 3535–3542 (2005).
18. M. J. Lockyear, A. P. Hibbins, J. R. Sambles, and C. R. Lawrence, "Surface-topography-induced enhanced transmission and directivity of microwave radiation through a subwavelength circular metal aperture," Appl. Phys. Lett. **84**, 2040–2042 (2004).
19. M. J. Lockyear, A. P. Hibbins, J. R. Sambles, and C. R. Lawrence, "Enhanced microwave transmission through a single subwavelength aperture surrounded by concentric grooves," J. Opt. A: Pure Appl. Opt. **7**, S152–S158 (2005).
20. H. Caglayan, I. Bulu, and E. Ozbay, "Extraordinary grating-coupled microwave transmission through a subwavelength annular aperture," Opt. Express **13**, 1666–1671 (2005).
21. H. Caglayan, I. Bulu, and E. Ozbay, "Beaming of electromagnetic waves emitted through a subwavelength annular aperture," J. Opt. Soc. Am. B **23**, 419–422 (2006).
22. T. Ishi, J. Fujikata, K. Makita, T. Baba, and K. Ohashi, "Si nano-photodiode with a surface plasmon antenna," Jpn. J. Appl. Phys. **44**, L364–L366 (2005).
23. Z. Yu, G. Veronis, S. Fan, and M. L. Brongersma, "Design of midinfrared photodetectors enhanced by surface plasmons on grating structures," Appl. Phys. Lett. **89**, 151116 (2006).
24. D. M. Schaadt, B. Feng, and E. T. Yu, "Enhanced semiconductor optical absorption via surface plasmon excitation in metal nanoparticles," Appl. Phys. Lett. **86**, 063106 (2005).
25. N. C. Panoiu and R. M. Osgood, "Enhanced optical absorption for photovoltaics via excitation of waveguide and plasmon-polariton modes," Opt. Lett. **32**, 2825 (2007).
26. A. Yariv, *Optical Electronics in Modern Communications* (Oxford University Press, New York, 1997), chap. 11, 5th ed.
27. A. Taflove and S. C. Hagness, *Computational Electrodynamics: The Finite-Difference Time-Domain Method* (Artech House, Boston, 2005), 3rd ed.
28. RSoft Design Group, FullWAVE™ 6.0.2, http://www.rsoftdesign.com/.
29. J. B. Pendry, L. Martín-Moreno, and F. J. García-Vidal, "Mimicking surface plasmons with structured surfaces," Science **305**, 847–848 (2004).
30. A. Roberts, "Electromagnetic theory of diffraction by a circular aperture in a thick, perfectly conducting screen," J. Opt. Soc. Am. A **4**, 1970–1983 (1987).
31. F. J. García de Abajo, "Light transmission through a single cylindrical hole in a metallic film," Opt. Express **10**, 1475–1484 (2002).
32. S. H. Zaidi, M. Yousaf, and S. R. J. Brueck, "Grating coupling to surface plasma waves. I. First-order coupling," J. Opt. Soc. Am. B **8**, 770–779 (1991).
33. O. T. A. Janssen, H. P. Urbach, and G. W. 't Hooft, "Giant optical transmission of a subwavelength slit optimized using the magnetic field phase," Phys. Rev. Lett. **99**, 043902 (2007).
34. D. A. Thomas and H. P. Hughes, "Enhanced optical transmission through a subwavelength 1d aperture," Solid State Commun. **129**, 519–524 (2004).
35. F. J. García-Vidal, H. J. Lezec, T. W. Ebbesen, and L. Martín-Moreno, "Multiple paths to enhance optical transmission through a single subwavelength slit," Phys. Rev. Lett. **90**, 213901 (2003).
36. W. L. Barnes, A. Dereux, and T. W. Ebbesen, "Surface plasmon subwavelength optics," Nature (London) **424**, 824–830 (2003).
37. L. Tang, D. A. B. Miller, A. K. Okya, J. A. Matteo, Y. Yuen, K. C. Saraswat, and L. Hesselink, "C-shaped nanoaperture-enhanced germanium photodetector," Opt. Lett. **31**, 1519–1521 (2006).

#91481 - $15.00 USD Received 8 Jan 2008; revised 19 Feb 2008; accepted 20 Feb 2008; published 19 Mar 2008

1. Introduction

It has been established that the transmission of light through a hole (or a slit) in a metal film can be enhanced by microstructuring of the top surface of the film with a grating; the grating couples incident light to surface plasmon polaritons (SPPs), which are guided into the hole [1–15]. Separate, but related observations of this enhancement have been made at THz [16, 17] and microwave [18–21] frequencies. This same phenomenon can also enhance absorption in a dielectric material inside or beneath the hole [22, 23] or in similar geometries important for photodetection and photovoltaic applications [24, 25]. In effect, the grating acts as an antenna to collect and concentrate the signal into a reduced detector volume, which can increase the signal-to-noise ratio (S/N) and/or speed of the detector. To that end, Ishi *et al*., showed that the photocurrent of an optical detector with subwavelength dimensions can be increased by several tenfold when surrounded by a circular metal grating [22].

To increase S/N in the context of a pixel in a detector array however, one must consider the area of the grating as well. Since S/N generally increases with increased detector area, an improved detector design must have a larger S/N ratio than a detector with an exposed surface area as large as the entire grating. We define a figure of merit F equal to the S/N for the grating detector divided by the S/N for a comparable detector but with the entire top metal surface removed. As we demonstrate below, enhanced absorption compared to a metal film with a hole and no grating is not a sufficient condition for achieving $F > 1$, and in fact previously proposed detector designs do not achieve $F > 1$ [22, 23]. In this paper, we optimize grating parameters to show that it is indeed possible to increase the signal-to-noise ratio of a photodetector pixel using a metal grating.

The dominant source of noise in typical infrared photodetectors, especially when they are uncooled, is thermal generation-recombination noise in photoconductors or shot noise of dark current in photovoltaic detectors [26]. These noise sources are proportional to the square root of the surface area of the detection volume [26]. Consider two photodetector pixels made with identical material parameters, each of total surface area G, the first having a detection volume with surface area G, and the second having a smaller detection volume with surface area A surrounded by a metal grating. The first detector has signal-to-noise ratio $S_1/N_1 \propto \sqrt{G}(1-R_1)$, where R_1 is the reflectivity of the detector. We can estimate the power absorbed in the second photodetector by assuming that it is proportional to AT_{AN}, where T_{AN} is the area-normalized-transmission (i.e., the transmission of the grating normalized by the power incident on the area A), so that $S_2/N_2 \propto T_{\mathrm{AN}}\sqrt{A}$. Thus the figure-of-merit for signal-to-noise improvement for the grating is $F \equiv (S_2/N_2)/(S_1/N_1) \approx \sqrt{A/G}T_{\mathrm{AN}}/(1-R_1)$, assuming the ratio of the proportionality constants is of order unity. This argument demonstrates that to achieve $F > 1$ one requires a grating with area-normalized transmission larger than $\sqrt{G/A}$.

To demonstrate the feasibility of such a scheme for infrared photodetection, we calculate the absorption for a circular (bull's eye) grating in a metal film on a dielectric substrate with parameters chosen so that the absorption is enhanced at a wavelength λ in the long-wavelength infrared (LWIR) near $10\,\mu$m. The system is sketched in Fig. 1 for a grating with 5 periods. Periodic gratings have been shown to give larger enhanced transmission than non-periodic gratings [14, 19] (although non-periodic Bessel gratings are optimal for Bessel beams [10]). Surface waves excited on the grating propagate towards a small detector volume. We compare circular gratings, which have a cross-section as shown in Fig. 1, and linear gratings, which are uniform in the direction perpendicular to Fig. 1. Circular gratings have two advantages over linear gratings. First, they have an inherently polarization-independent response at normal incidence and second, as we will show below, the circular geometry focusses light more efficiently than the linear geometry.

#91481 - $15.00 USD Received 8 Jan 2008; revised 19 Feb 2008; accepted 20 Feb 2008; published 19 Mar 2008

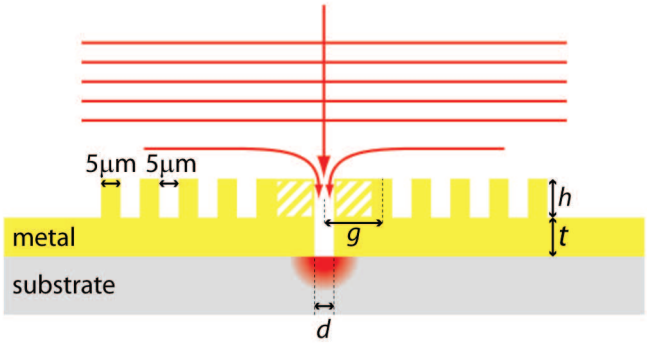

Fig. 1. Schematic cross-section for a 5-period grating; a plane wave incident from above is collected over the large area of the grating (height h) and coupled through the hole (diameter d, depth t) to be absorbed in the substrate. The parameter g is measured from the center of the hole to the center of the first grating tooth. In the case of a circular grating, there is cylindrical symmetry about a line through the center, whereas in the case of a linear grating, there is translational invariance in the direction perpendicular to the figure. We show below that absorption is larger when the hatched areas are air rather than metal.

2. Method

We solve Maxwell's equations for the electromagnetic field using a total-field / scattered-field formulation of the finite-difference time-domain (FDTD) method with perfectly matched layer (PML) boundary conditions [27]. The FDTD method solves the full Maxwell's equations directly in the time domain, and so all evanescent surface waves and propagating fields are automatically included in the calculation; details of the method are given, for example by Taflove and Hagness [27]. We exploit the cylindrical symmetry of the circular grating to reduce computational demand by using radial FDTD [6, 13, 14]; we have validated the cylindrically symmetric FDTD code by replicating selected results with a separate 3D-FDTD code (both are part of the commercially available FullWAVE [28]). A linearly polarized, short pulse plane wave is normally incident on the grating, and we calculate the frequency transform of the power absorbed in the substrate and of the power transmitted through the hole. This method gives the steady state response that would result from continuous wave excitation at each frequency. For the linear grating, the incident electric field is polarized in the direction across the slit (TM polarization). The calculations are well-converged with a 50 nm grid and a total simulation time of a few picoseconds. Reflection of evanescent surface waves from the PML can be avoided either by expanding the computational domain in the z-direction (normal to the grating) or using an improved PML [27]. In the transverse direction, we have used a computational domain wide enough so that surface waves excited from the edge of the metal film do not reach the hole before the computation is stopped; however, in many cases the absorption enhancement is large enough that the edge effects of a narrower domain are insignificant. We model the metal as having an index of refraction with effectively infinite imaginary part, and zero real part, which is an excellent approximation due to the short skin depth in the LWIR range, and we treat the substrate as a model dielectric with frequency-independent index of refraction 3.57, extinction coefficient 0.21, and 200 nm thickness; these parameters are, for example, a reasonable approximation to HgCdTe-based detector materials. Our simulations show that all of the power absorbed in the substrate is absorbed in a volume with diameter less than twice the diameter of the hole. This was determined by varying the diameter of the volume in which absorption was

#91481 - $15.00 USD Received 8 Jan 2008; revised 19 Feb 2008; accepted 20 Feb 2008; published 19 Mar 2008

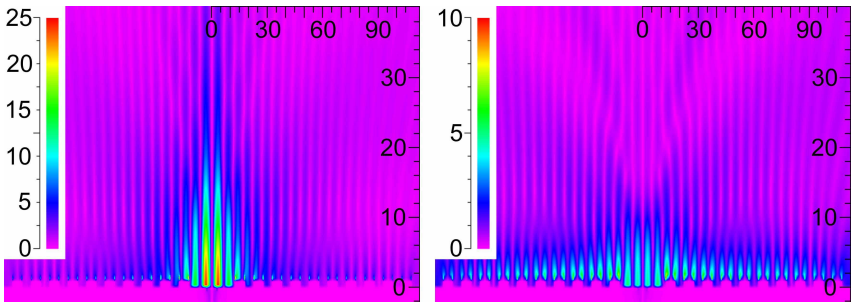

Fig. 2. Amplitude of the normal component of the electric field for 10-period circular (left) and linear (right) antenna at the resonant frequency for each grating (wavelength $\lambda = 10.2\,\mu$m for circular grating and $\lambda = 10.6\,\mu$m for linear grating). In each cases the grating period is $\Lambda = 10\,\mu$m, grating height is $1.35\,\mu$m, grating duty cycle is 0.5, hole depth is $0.1\,\mu$m, hole diameter is $5\,\mu$m, and $g = 1.5\Lambda$. The field amplitude is scaled relative to the magnitude of the incident field. The horizontal and vertical axes are labeled in μm units.

monitored. As the diameter of the absorption monitor was increased, the measured absorbed power increased, but it had converged for a diameter of twice the diameter of the hole, and indeed most of the power is absorbed in a diameter equal to the diameter of the hole.

3. Results

The excitation of a surface wave when light is incident on the grating can be seen clearly in Fig. 2, which shows for two particular grating geometries the magnitude of the normal component of the electric field, $|E_z|$, at the resonant frequency of each grating. Note that since we have effectively used an infinite conductivity, these surface waves are so-called "spoof surface plasmons" rather than true SPPs [29]. (In Ref. [29], the properties of these spoof plasmons were investigated in the limit case of a structured surface with period that is much smaller than the wavelength; however, the existence of such plasmon modes is not necessarily restricted to this particular case.) The spatial distributions of the excited surface waves and the radiated power are different for circular and linear gratings. In the circular grating, the surface waves are focussed in the center leading to much stronger fields in the detector volume. In contrast the linear grating excites surface waves uniformly along the length of the grating. Note that the color scales in the two panels of Fig. 2 are different; in the circular grating, $|E_z|$ is up to 24 times as large as the incident field in the inner portion of the grating and up to 6 times as large in the outer portion of the grating, whereas $|E_z|$ in the linear grating is generally more uniform and is at most 10 times as large as the incident field. Note that although $|E_z|$ is useful for visualizing the surface waves, it has a small magnitude inside the hole where transverse electric fields dominate.

In this paper, to simplify our presentation, we consider circular gratings with a simple hole (i.e., not a coaxial hole [6] or a hole filled with a dielectric [14]). Area-normalized transmission through a simple hole without a grating is maximal for a hole diameter close to the cutoff diameter for propagating modes in the hole; at this maximum, most of the energy is transmitted by evanescent modes in the hole, and hence the transmission decreases monotonically with increased hole depth [30, 31]. Thus we fix the depth of the hole at $0.1\,\mu$m (we use a hole diameter of $5\,\mu$m except where noted below); using a hole ten times deeper decreases the absorbed power by $> 30\%$.

#91481 - $15.00 USD Received 8 Jan 2008; revised 19 Feb 2008; accepted 20 Feb 2008; published 19 Mar 2008

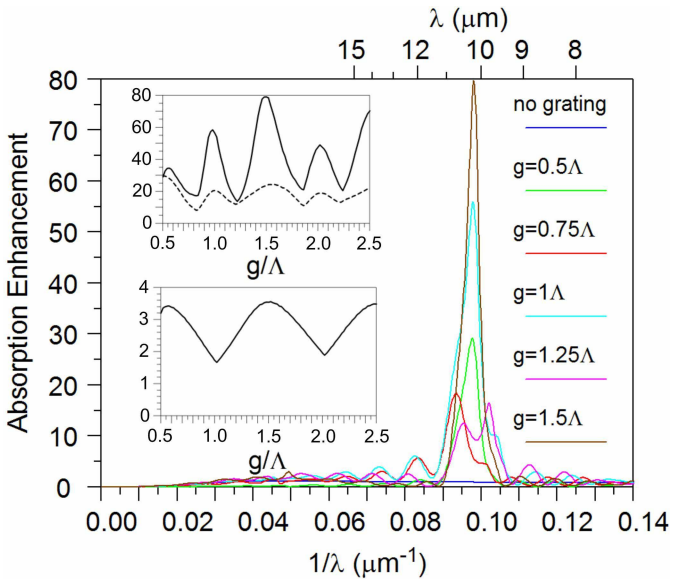

Fig. 3. Spectrum of absorption for 10-period circular grating for various values of g, the distance between the grating and the hole. The spectra are normalized to the $\lambda = 10.2\,\mu$m absorption in the case of a metal film with a hole but no grating. Upper inset: peak absorption as a function of g with hatched area in Fig. 1 as air (solid line) or metal (dashed line). Lower inset: similar to solid line in upper inset, but grating height $h = 200$ nm. $\Lambda = 10\,\mu$m is the grating period.

We have used our calculation to optimize several parameters of the grating design. First, we have found that a grating height, h, of $1.35\,\mu$m maximizes the photodetector absorption for a 10-period grating when other parameters are held at their optimal values. A shallower grating couples the incident light less efficiently into the grating, whereas a deeper grating couples the grating surface waves more extensively into radiation and is therefore less efficient at coupling light into the detector well [32]. Note that when scaled by the wavelength, our optimal grating height is comparable to grating heights that have been optimized for other wavelength regimes [13, 19]. Second, we have found that the photodetector absorption is optimized with a grating duty cycle of 0.5 (equal ridge and groove widths). This is in contrast to the results of Lockyear *et al*. [19], but similar to what has been found for some other geometries [14, 33].

In our simulations, we have found that the spacing between the grating and the central hole, g in Fig. 1, has an important effect on the absorption in the central photodetector volume. In particular it affects the phase relationship between the grating-induced surface wave and the directly incident light in the central region of the structure [8, 14, 16]. In Fig. 3, we plot spectral response for 10-period circular gratings with various values of g, as well as the spectral response for a metal film with a hole but no grating ($h = 0$). The photodetector response peaks at an incident wavelength of $10.2\,\mu$m, which is slightly larger than the grating period $\Lambda = 10\,\mu$m due to the dispersion of SPPs. With $h = 0$, the absorption at wavelength $\lambda = 10.2\,\mu$m is 0.049 times the power incident on the area of the hole, which corresponds to about 6% of the power transmitted through the hole. We define the *absorption enhancement* as the absorption relative to this value. (To connect with the approximate formula for F given above, the grating T_{AN} is approximately the absorption enhancement times the T_{AN} of a bare hole with no grating, which is 0.79 at $\lambda = 10.2\,\mu$m; also, $R_1 = 0.34$.) The case $g = 1.5\Lambda$ produces the largest absorption

#91481 - $15.00 USD Received 8 Jan 2008; revised 19 Feb 2008; accepted 20 Feb 2008; published 19 Mar 2008

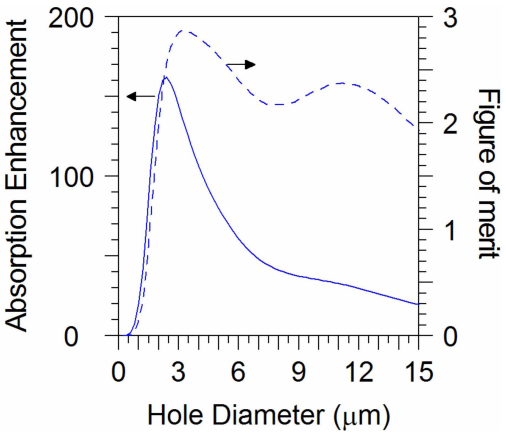

Fig. 4. Varying hole diameter for a 10-period circular grating. Solid line is absorption enhancement, dashed line is the S/N enhancement figure-of-merit F.

peak, having an absorption enhancement of 80. The dependence of the peak height on g is shown in the solid line of the upper inset of Fig. 3; varying g in the range shown can increase the peak absorption by almost 5 times, thus this quantity is an important parameter for designing an efficient collection system. For shallow gratings, the dependence of the peak absorption on g is close to the more intuitive sinusoidal dependence (except for a deviation near $g = 0$, since in that case the hole is effectively deeper); this is shown in the lower inset of Fig. 3 for a grating with $h = 0.2\,\mu$m.

A seemingly minor feature of grating design, which has important consequences for collection efficiency [34], is the thickness of the metal film in the central region between the innermost part of the grating and the hole. Such a region, shown by hatched rectangles in Fig. 1, exists when g is larger than half a period. In other studies of SPP collection, the film thickness in this region was fixed either to the reach of the tops of the grating [8, 14] or countersunk [18, 19]. We have examined a variety of thicknesses and found that when the central region is "low" (i.e., has a thickness equal to that in the grating grooves) the absorption enhancement is 3.3 times larger than when the central region is "high" (i.e., has a thickness equal to that in the grating ridges). The peak absorption enhancements for "low" and "high" central regions are compared in the upper inset of Fig. 3. Note that when the central region is "high" the hole is deeper, but that the decrease in absorption is not simply due to the difference in hole depth since a grating with "low" central region and hole depth t matched to the "high" case is still 1.8 times larger than the "high" case. Moreover the difference cannot be accounted for by adding an extra period to the grating in the "high" case, which only increases the absorption by 16%. In fact, the difference must be due to improved coupling of the surface wave from the grating to the hole when the flat region is "low".

A subtle, but important parameter for improving S/N in a photodetector is the central hole diameter. Since the hole diameter appears directly in the approximate formula for the S/N figure of merit F, the absorption enhancement and F should not peak at the same hole diameter. Figure 4 shows the dependence of absorption enhancement and S/N enhancement factor (F) on the hole diameter. In an earlier transmission study, Thio *et al*. found that area-normalized transmission at optical frequencies is roughly independent of hole diameter [2]. In contrast, we find that as the hole size is increased, more power is absorbed but the increase is not proportional to the hole area. In our case, the absorption enhancement peaks at a diameter of $2.4\,\mu$m. For

#91481 - $15.00 USD Received 8 Jan 2008; revised 19 Feb 2008; accepted 20 Feb 2008; published 19 Mar 2008

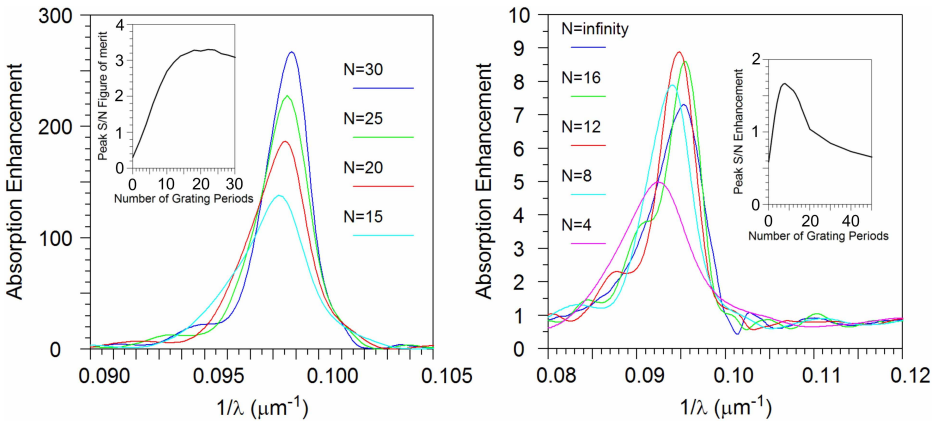

Fig. 5. Varying number of grating periods, N, for a circular grating (left) and linear grating (right) with parameters as in Fig. 2. The main plots show the spectral response of the absorption enhancement, and the insets show the F for the wavelengths corresponding to the peaks in the spectral response.

holes with $d < 2.4$ the power throughput decreases sharply, while for larger holes the power throughput decreases weakly in an oscillatory manner. This is similar to the dependance on hole diameter of a bare hole [31]. Such a connection between the results for a bare hole and a hole with a grating is reminiscent of the overlapping of waveguide resonances and SPP resonances in the linear grating geometry [35]. The figure of merit F, shown as the dashed line in Fig. 4, peaks at a hole diameter of about $3.3\,\mu$m, and is weakly dependent on diameter for larger holes (at $d = 5\,\mu$m, which was used in the rest of the calculations in this paper, F is 6% smaller).

As the number of grating periods N increases, the absorption enhancement of the detector should increase as the grating collects additional optically excited surface waves; however, a saturation point will be reached when additional collection is balanced by re-radiation. The finite conductivity of real metals, which causes a finite SPP propagation length, could also limit grating collection in principle, although it is not the limiting factor here, since the SPP propagation length of a flat, real metal surface is on the order of 1 cm at a wavelength of $10\,\mu$m [36]. Prior experimental and theoretical studies of enhanced transmission or absorption through a hole with a circular grating have typically examined only a small number of grating periods (up to 16) [1–15,22]. We have simulated photodetectors with up to 30 grating periods. The results, shown in Fig. 5, are striking. They show that the absorption enhancement of the circular grating continues to grow with the number of periods up to an absorption enhancement of almost 270, which corresponds to a figure of merit F over 3. In contrast the absorption enhancement for a linear grating of the same dimensions peaks at 13 grating periods with an absorption enhancement of only 9; moreover, it saturates by $N = 20$. For different grating dimensions, García-Vidal *et al*. and Yu *et al*. found saturation at $N \approx 15$, and $N \approx 20$, respectively [23, 35].

The overall grating size also appears directly in the approximate formula for the S/N figure of merit F; due to the additional factor $1/\sqrt{G}$, F peaks for smaller grating periods than the absorption enhancement. As shown in Fig. 5, the circular grating reaches a maximum F of 3.3 for a 22-period grating, even though the absorption enhancement has not saturated for gratings up to 30 periods, which for circular gratings is the limit of our computational resources. The linear grating reaches a maximum F of 1.7 for an 8-period grating. Note that even though absorption enhancement of a circular grating is more than an order of magnitude larger than that of a comparable linear grating, the figure of merit F is only twice as large. This is because

#91481 - $15.00 USD Received 8 Jan 2008; revised 19 Feb 2008; accepted 20 Feb 2008; published 19 Mar 2008

the detector size to grating size ratio, A/G, is larger for linear gratings.

The results plotted in Fig. 5 are for a constant grating depth of $1.35\,\mu$m, which maximizes the absorption of the 10-period circular grating. In general, the optimal grating depth depends on the number of grating periods; as N increases, the optimal h decreases [33]. According to our FDTD simulations, the 30-period linear grating response is largest for $h = 0.75\,\mu$m, for which the absorption enhancement is 14 and $F = 1.6$; note that this is still less than the F for the 8-period grating. The 30-period circular grating response is largest for $h = 1\,\mu$m, for which the absorption enhancement is 436 and $F = 5.2$. Thus larger circular gratings with optimized grating depth could have even larger F.

4. Conclusion

We have shown, by introducing the figure of merit F, that it is in fact possible to design a metal grating so that S/N can be enhanced compared to that in a larger photodetector without a metal grating, which is the relevant comparison in the context of a detector array. Other measures, such as area-normalized transmission and absorption enhancement have larger absolute values, but can be misleading if one is interested exclusively in enhancing the S/N ratio (as opposed to detector speed, which can also be improved with the grating design discussed here). Ishi *et al*. used a grating to enhance the speed of a Si photodetector and found an absorption enhancement of between 10 and 20 with a device having $\sqrt{A/G} = 0.026$ [22]. To achieve an impressive increase in detector speed, the bare hole T_{AN} is relatively small in their experiment, which implies a S/N figure of merit for their detector that is much less than 1. Yu *et al*. proposed using a linear grating with the detector material inside the slit. Their design, which has $\sqrt{A/G} = 0.011$, exploited a Fabry-Perot resonance in the slit to achieve 250 times more absorption than in a region of detector material as large as the slit. This implies a figure of merit $F = 2.75$. Such resonances could also be exploited in a circular geometry by using more complicated hole shapes [6, 37] or by filling the hole with a dielectric [14], which could lead to even larger figures of merit than we have presented here with a simple hole.

In summary, we have identified and optimized relevant grating parameters for circular and linear gratings with a simple hole/slit and shown with FDTD simulations that a circular grating more efficiently channels plasmon surface waves into the hole compared to a linear grating leading to a superior S/N enhancement. Note that we have not examined the linewidth or angular dependence of the spectral response in this paper.

Acknowledgments

SB acknowledges funding from DARPA HOT MWIR program. The Columbia portion was supported by AFOSR STTR FA9550-05-C-1954 and AFOSR/DARPA FA9550-05-1-0428. We thank M. Bahl and R. Scarmozzino of RSoft for several important suggestions.

#91481 - $15.00 USD Received 8 Jan 2008; revised 19 Feb 2008; accepted 20 Feb 2008; published 19 Mar 2008